

Dynamics of a thin shell in the Reissner–Nordström metric

V. I. Dokuchaev^{1,*} and S. V. Chernov^{1,2,†}

¹*Institute for Nuclear Research, Russian Academy of Sciences,
pr. 60-letiya Oktyabrya 7a, Moscow, 117312 Russia*

²*Lebedev Physical Institute, Russian Academy of Sciences, Leninskii pr. 53, Moscow, 119991 Russia*

We describe the dynamics of a thin spherically symmetric gravitating shell in the Reissner–Nordström metric of the electrically charged black hole. The energy-momentum tensor of electrically neutral shell is modelled by the perfect fluid with a polytropic equation of state. The motion of a shell is described fully analytically in the particular case of the dust equation of state. We construct the Carter–Penrose diagrams for the global geometry of the eternal black hole, which illustrate all possible types of solutions for moving shell. It is shown that for some specific range of initial parameters there are possible the stable oscillating motion of the shell transferring it consecutively in infinite series of internal universes. We demonstrate also that this oscillating type of motion is possible for an arbitrary polytropic equation of state on the shell.

PACS numbers: 04.20.-q 04.70.-s 98.80.-k

I. INTRODUCTION

The model of thin gravitating shells that was first proposed by Israel [1] occupies an important place among the exactly solvable problems in general relativity. The formalism of the model of thin shells was subsequently developed in details and used for a wide class of cosmological and astrophysical problems [2–6]. In particular, when the phase transitions in the early universe are analyzed [7, 8], the model of thin shells is a very convenient formalism that allows the dynamics of the phase transitions themselves and the formation and evolution of baby universes to be traced in sufficient detail [9–25]. The phase transitions in the early universe begin with the formation of seed bubbles of a new vacuum [26–30]. This process is a quantum one, but the bubbles of a new vacuum pass into the classical stage of evolution due to their rapid expansion. The classical stage of dynamical evolution of vacuum bubbles was considered using the formalism of thin shells in many papers [5, 6, 31–40]. In astrophysics, the formalism of thin shells helps to analyze the relativistic properties of compact stellar systems [41]. In the field theory, models similar to the model of a thin shell were constructed when the decay dynamics of a metastable vacuum was studied [7, 8, 26–30, 42–45]. The model of thin shells is also convenient for the semiclassical description of quantum black holes [46–52]. The special case of a thin shell with a phantom equation of state falling to a black hole was considered in [53]. The dynamics of a thin rotating dust shell was studied in [54].

The possibility of a stable (oscillatory) motion of a shell in the metric of an electrically charged Reissner–Nordström black hole was recently discussed in [55]. However, the corresponding solution was not found. A spherically symmetric shell in the Minkowski [32], Schwarzschild [2, 6], Schwarzschildde Sitter [5, 40] metrics, and the Friedmann–Schwarzschild universe [39] is known to be dynamically unstable. In the long run, the shell either collapses (falls to the central singularity) or expands infinitely. In this paper, we investigate in detail the dynamics of a spherically symmetric shell for the Reissner geometry and find the conditions under which the shell oscillations can be stable. In particular, this problem can be investigated completely analytically for a dust shell. Kuchar [3] was among the first authors who considered the problem on the dynamical evolution of a shell in the Reissner metric. In particular, he showed that the electric charge of the black hole could prevent the shell collapse, i.e., a bounce point could exist. Previously, Novikov [56] showed that the collapse of a charged sphere could stop and subsequently expand into another universe. The existence of a bounce point for a contracting shell can provide its oscillatory motion in the case of an eternal black hole whose global geometry contains an infinite number of identical universes. This possibility was discussed qualitatively in [55]. Below, we will find necessary conditions for the realization of such an oscillatory shell motion and the corresponding exact analytical solution. The same oscillatory shell motion can be assumed to be possible for the Kerr metric, because a rotating black hole has a centrifugal barrier. There is no such possibility for a Schwarzschild black hole and the collapsing shell inevitably falls to the central singularity.

*Electronic address: dokuchaev@ms2.inr.ac.ru

†Electronic address: chernov@lpi.ru

Everywhere below, we assume that the Greek indices α, β, \dots correspond to four coordinates t, r, θ and φ in the four dimensional spacetime, while the Latin indices i, k, \dots correspond to three coordinates t, θ and φ on the shell.

II. THE EQUATIONS OF MOTION OF THE SHELL

Let there be a spherically symmetric hypersurface Σ in the four dimensional spacetime that divides the spacetime into two regions. We will denote the inner and outer parts by the subscripts "in" and "ou". We will describe each region inside and outside this hypersurface by the metric of an electrically charged Reissner–Nordström black hole. It has the well known form

$$ds_{\text{in,out}}^2 = \left(1 - \frac{2m_{\text{in,out}}}{r} + \frac{Q_{\text{in,out}}^2}{r^2}\right) dt^2 - \left(1 - \frac{2m_{\text{in,out}}}{r} + \frac{Q_{\text{in,out}}^2}{r^2}\right)^{-1} dr^2 - r^2 d\Omega,$$

where $m_{\text{in,out}}$ are the black hole masses and $Q_{\text{in,out}}$ are the electric charges inside and outside the hypersurface Σ . Since we will consider an electrically neutral spherical shell, $Q_{\text{in}} = Q_{\text{out}} = Q$. By spherical symmetry, the metric on the shell is [6]

$$ds_{\Sigma}^2 = d\tau^2 - \rho^2(\tau)d\Omega, \quad (1)$$

where τ is the proper time of an observer located on the shell and ρ is the shell radius measured by the observer on the shell. The equations of motion of a thin shell were derived in many papers (see, e.g., [6]) and can be written as

$$\begin{aligned} [K_0^0] + [K_2^2] &= 8\pi S_2^2, & \{K_0^0\}S_0^0 + 2\{K_2^2\}S_2^2 + [T_n^n] &= 0, \\ [K_2^2] &= 4\pi S_0^0, & \frac{dS_0^0}{d\tau} + \frac{2\dot{\rho}}{\rho}(S_0^0 - S_2^2) + [T_0^0] &= 0, \end{aligned} \quad (2)$$

where K_i^j is the extrinsic curvature, T_α^β is the energy momentum tensor of matter inside and outside the shell, S_i^j is the energymomentum tensor of the shell itself, and the following notation is used: $[T] = T_{\text{out}} - T_{\text{in}}$ and $\{T\} = T_{\text{out}} + T_{\text{in}}$. The expressions for the extrinsic curvature in the Reissner–Nordström metric are [3, 6]

$$K_2^2 = -\frac{\sigma}{\rho} \sqrt{\rho^2 + 1 - \frac{2m}{\rho} + \frac{Q^2}{\rho^2}}, \quad K_0^0 = -\sigma \frac{\ddot{\rho} + m/\rho^2 - Q^2/\rho^3}{\sqrt{\rho^2 + 1 - 2m/\rho + Q^2/\rho^2}}, \quad (3)$$

where $\sigma = \pm 1$. It can be shown [57] that the signs of σ coincide with those of the R_+ and R_- spacetime regions. A charged black hole produces an electric field outside the black hole whose electromagnetic field tensor is [58]

$$F_{tr} = \frac{Q}{r^2} = -F^{tr}. \quad (4)$$

The corresponding energymomentum tensor of the electromagnetic field is

$$4\pi T_\beta^\alpha = -F^{\alpha\gamma}F_{\beta\gamma} + \frac{1}{4}\delta_\beta^\alpha F_{\gamma\delta}F^{\gamma\delta}, \quad T_t^t = T_r^r = -T_\theta^\theta = -T_\varphi^\varphi = \frac{1}{8\pi} \frac{Q^2}{r^4}. \quad (5)$$

The corresponding formulas of the passage to the limit [6] should be used to calculate the energymomentum tensor on a thin shell. As a result, we obtain.

$$T_0^n = n_{,t} \frac{\partial t}{\partial \tau} T_t^t + n_{,r} \frac{\partial r}{\partial \tau} T_r^r = 0, \quad T_n^n = T_t^t. \quad (6)$$

We will consider a shell model with the energy momentum tensor of an ideal fluid,

$$S_{ij} = (p + \mu)u_i u_j - pg_{ij}, \quad (7)$$

where p is the pressure in the fluid and μ is its total energy density. In the reference frame of an observer located on the three dimensional shell under consideration, the fluid velocity components are $u_i = (1, 0, 0)$. For an ideal fluid, the relations $S_0^0 = \mu$, $S_2^2 = S_3^3 = -p$ also hold.

Consider a polytropic equation of state $p = kn^\gamma$, where n is the number density and γ is the polytropic index. The total energy density for the polytropic equation of state is $\mu = n + p/(\gamma - 1)$, where the first and second terms

correspond to the fluid particle rest mass and the internal energy density, respectively [59]. In particular, $p = 0$ and $\mu = n$ for dust; for thermal radiation, the fluid particle rest mass is zero, $\gamma = 4/3$, and $\mu = 3p$; for the special case of $\gamma = 2$, $\mu = n + p$. This equation of state for $p \gg n$ reproduces the ultra-stiff equation of state of a fluid in which the speed of sound is equal to the speed of light [60]: $\mu = p$. For the polytropic equation of state under consideration, we find the dependence of the number density n on the shell radius ρ measured by an observer on the shell using the last equation in (2):

$$n = \frac{A}{\rho^2}. \quad (8)$$

Here, A is the constant of integration. Accordingly, the dependence of the total energy density S_0^0 on the shell radius ρ is

$$S_0^0 = \mu(\rho) = \frac{A}{\rho^2} + \frac{k}{\gamma - 1} \frac{A^\gamma}{\rho^{2\gamma}}. \quad (9)$$

As a result, the first equation in (2), which describes the shell dynamics, will be written in final form as

$$\sigma_{\text{in}} \sqrt{\dot{\rho}^2 + 1 - \frac{2m_{\text{in}}}{\rho} + \frac{Q^2}{\rho^2}} - \sigma_{\text{out}} \sqrt{\dot{\rho}^2 + 1 - \frac{2m_{\text{out}}}{\rho} + \frac{Q^2}{\rho^2}} = 4\pi\rho\mu(\rho), \quad (10)$$

where $\sigma_{\text{in},\text{out}} = \pm 1$. It is this equation that we will investigate by assuming that $\mu(\rho) > 0$.

For the subsequent analysis, it is convenient to rewrite Eq. (10) as the ‘‘energy conservation law’’ by separating out the kinetic and potential parts. Squaring Eq. (10) yields the equation

$$m_{\text{out}} = m_{\text{in}} + 4\pi\rho^2\mu\sigma_{\text{in}}\sqrt{\dot{\rho}^2 + 1 - \frac{2m_{\text{in}}}{\rho} + \frac{Q^2}{\rho^2}} - 8\pi^2\rho^3\mu^2. \quad (11)$$

The quantity m_{out} in this equation is treated as the Hamiltonian of the entire system [51] (see also [52]) and is the total energy of the entire system that is conserved during the dynamical evolution of the shell. It is easy to assign a physical meaning to other terms in this equation [5, 6]. The first term is the intrinsic mass of the inner black hole. The second term has the meaning of kinetic energy and the third term is the gravitational energy of a self-interacting shell with radius ρ . We will call the surface density of this energy an effective tension of the shell. The Coulomb energy does not enter into Eq. (11), because the shell considered here is electrically neutral. Nevertheless, the electric charge of the black hole enters into the term for the kinetic energy, because it contributes to the gravitational field of the black hole. Squaring Eq. (11) once again yields an equation for the shell evolution in a form convenient for the subsequent analysis:

$$\dot{\rho}^2 + U = 0, \quad (12)$$

where the effective potential $U = U(\rho)$ is

$$U = 1 + \frac{Q^2}{\rho^2} - \frac{m_{\text{out}} + m_{\text{in}}}{\rho} - 4\pi^2\rho^2\mu^2(\rho) - \frac{(m_{\text{out}} - m_{\text{in}})^2}{16\pi^2\rho^4\mu^2(\rho)}. \quad (13)$$

The conditions on the signs of σ_{out} and σ_{in} that can be obtained using Eq. (10): should also be added to this equation:

$$\sigma_{\text{out}} = \text{sign} \left[m_{\text{out}} - m_{\text{in}} - 8\pi^2\rho^3\mu^2(\rho) \right], \quad (14)$$

$$\sigma_{\text{in}} = \text{sign} \left[m_{\text{out}} - m_{\text{in}} + 8\pi^2\rho^3\mu^2(\rho) \right]. \quad (15)$$

In the next section, we investigate these equations in detail for a dust shell. Similar analysis for other metrics were performed in many papers [5, 39, 40]. Below, using the Carter–Penrose diagrams, we will construct the global geometries of the configuration of a charged black hole and a moving shell under consideration by assuming the black hole to exist eternally. It is on these diagrams that the entire evolutionary history of the shell can be traced most completely. The initial Carter–Penrose diagram for the global geometry of an eternally existing Reissner–Nordström black hole without a shell is shown in Fig. 1.

III. A DUST SHELL

We will begin our consideration of the shell dynamics with the simplest case where the shell is a dust one, i.e., the pressure in it is zero and the energy density is $\mu(\rho) = A/\rho^2$ (see (8) and (9)). For a dust shell, the effective potential U in the equation of motion of the shell (12) is simplified considerably and takes the form

$$U = 1 + \frac{Q^2}{\rho^2} - \frac{m_{\text{out}} + m_{\text{in}}}{\rho} - \left(\frac{m_{\text{out}} - m_{\text{in}}}{4\pi A} \right)^2 - 4\pi^2 \frac{A^2}{\rho^2}. \quad (16)$$

The corresponding conditions (14) and (15) for the signs of σ will be written as

$$\begin{aligned} \sigma_{\text{out}} &= \text{sign} \left[m_{\text{out}} - m_{\text{in}} - 8\pi^2 \frac{A^2}{\rho} \right], \\ \sigma_{\text{in}} &= \text{sign} \left[m_{\text{out}} - m_{\text{in}} + 8\pi^2 \frac{A^2}{\rho} \right]. \end{aligned} \quad (17)$$

The signs of σ_{out} and σ_{in} in these equations change when the shell reaches the radii ρ_{out} and ρ_{in} , respectively. These radii are

$$\rho_{\text{out}} = \frac{8\pi^2 A^2}{m_{\text{out}} - m_{\text{in}}}, \quad \rho_{\text{in}} = \frac{8\pi^2 A^2}{m_{\text{in}} - m_{\text{out}}}. \quad (18)$$

It can thus be easily seen that only one of the radii, ρ_{out} , exists at $m_{\text{out}} > m_{\text{in}}$, while in the opposite case, i.e., at $m_{\text{in}} > m_{\text{out}}$, only the second radius ρ_{in} exists. For the dust equation of state under consideration, we can find analytically all admissible solutions to the equation of motion of the shell (12) and classify all possible types of shell motion, which we will do below.

We will begin the classification of all possible types of motion of a dust shell by studying the characteristic features of the shape of potential (16). To find the extrema of this potential, let us calculate its first and second derivatives:

$$\frac{\partial U}{\partial \rho} = \frac{1}{\rho^2} \left[-\frac{2Q^2}{\rho} + m_{\text{in}} + m_{\text{out}} + \frac{8\pi^2 A^2}{\rho} \right], \quad (19)$$

$$\frac{\partial^2 U}{\partial \rho^2} = \frac{2}{\rho^3} \left[\frac{3Q^2}{\rho} - (m_{\text{out}} + m_{\text{in}}) - \frac{12\pi^2 A^2}{\rho} \right]. \quad (20)$$

We see from these equations that the existence or absence of a potential extremum depends on four characteristic quantities of our problem: m_{in} , m_{out} , Q and A . The value of the potential (16) at spacial infinity $\rho = \infty$ is

$$U(\infty) = 1 - \frac{(m_{\text{out}} - m_{\text{in}})^2}{16\pi^2 A^2}. \quad (21)$$

We see that the potential can be both positive and negative, depending on m_{out} , m_{in} and A . Accordingly, the existence or absence of bounce points outside the event horizon of a black hole will depend on the same parameters. Let us introduce compact designations for the characteristic outer and inner radii of the event horizons:

$$\rho_{\text{in}}^{\pm} = m_{\text{in}} \pm \sqrt{m_{\text{in}}^2 - Q^2}, \quad \rho_{\text{out}}^{\pm} = m_{\text{out}} \pm \sqrt{m_{\text{out}}^2 - Q^2}. \quad (22)$$

For the corresponding potentials at these shell radii, we will obtain

$$U(\rho_{\text{in}}^{\pm}) = - \left(\frac{2\pi A}{\rho_{\text{in}}^{\pm}} + \frac{m_{\text{out}} - m_{\text{in}}}{4\pi A} \right)^2, \quad (23)$$

$$U(\rho_{\text{out}}^{\pm}) = - \left(\frac{2\pi A}{\rho_{\text{out}}^{\pm}} - \frac{m_{\text{out}} - m_{\text{in}}}{4\pi A} \right)^2. \quad (24)$$

We can also see that the potential on the event horizons is always negative or zero. The potentials at the characteristic radii ρ_{out} and ρ_{in} are, respectively,

$$\begin{aligned} U(\rho_{\text{out}}) &= 1 - \frac{2m_{\text{out}}}{\rho_{\text{out}}} + \frac{Q^2}{\rho_{\text{out}}^2} - \left(\frac{2\pi A}{\rho_{\text{out}}} - \frac{m_{\text{out}} - m_{\text{in}}}{4\pi A} \right)^2, \\ U(\rho_{\text{in}}) &= 1 - \frac{2m_{\text{in}}}{\rho_{\text{in}}} + \frac{Q^2}{\rho_{\text{in}}^2} - \left(\frac{2\pi A}{\rho_{\text{in}}} + \frac{m_{\text{out}} - m_{\text{in}}}{4\pi A} \right)^2. \end{aligned} \quad (25)$$

It follows from these expressions that ρ_{out} and ρ_{in} coincide with the corresponding event horizons if the potential on the event horizons and at the characteristic radii ρ_{out} and ρ_{in} is zero. The potential is zero, $U = 0$, at the shell radius $\rho = \rho_0^\pm$, where

$$\rho_0^\pm = \frac{m_{\text{out}} + m_{\text{in}}}{2 \left[1 - \frac{(m_{\text{out}} - m_{\text{in}})^2}{16\pi^2 A^2} \right]} \left\{ 1 \pm \sqrt{1 - \frac{4(Q^2 - 4\pi^2 A^2)}{(m_{\text{out}} + m_{\text{in}})^2} \left[1 - \frac{(m_{\text{out}} - m_{\text{in}})^2}{16\pi^2 A^2} \right]} \right\}.$$

Using the equation for the first derivative of the potential, we can easily find the radius of its extremum

$$\rho_{\text{min}} = \frac{2(Q^2 - 4\pi^2 A^2)}{m_{\text{out}} + m_{\text{in}}}. \quad (26)$$

This extremum turns out to be a minimum. From the equation for zero of the second derivative of the potential, we will find the inflection point

$$\rho_{\text{inf}} = \frac{3(Q^2 - 4\pi^2 A^2)}{m_{\text{out}} + m_{\text{in}}} = \frac{3}{2} \rho_{\text{min}}. \quad (27)$$

At the extremum, the potential is

$$U(\rho_{\text{min}}) = 1 - \frac{(m_{\text{out}} - m_{\text{in}})^2}{16\pi^2 A^2} - \frac{(m_{\text{out}} + m_{\text{in}})^2}{4(Q^2 - 4\pi^2 A^2)} < 0.$$

It can be shown that the potential at the extremum is always negative.

For a more detailed description, let us consider a situation where $m_{\text{out}} > m_{\text{in}}$. The reverse situation is considered quite similarly. It can be shown that the inequality $\rho_{\text{out}}^+ > \rho_{\text{in}}^+ > \rho_{\text{in}}^- > \rho_{\text{out}}^-$ will hold at $m_{\text{out}} > m_{\text{in}}$. This inequality means that the inner (outer) event horizon of the metric under consideration under the shell is always larger (smaller) than the corresponding inner (outer) event horizon of the metric outside the shell. As a result, the parameter $\sigma_{\text{in}} = 1$ and the shell moves in this case in the R_+ spacetime of the inner part of the metric. Let us now consider the situation in which $m_{\text{out}} > m_{\text{in}}$ for several individual case.

First, let the case (I) where the inequalities $Q^2 > 4\pi^2 A^2$ ($m_{\text{out}} - m_{\text{in}})^2 > 16\pi^2 A^2$. hold be realized. The first inequality means that the branches of the potential U grow as the shell contracts radially and, hence, the shell will be unable to overcome the potential barrier. In other words, a bounce point $\rho_0^- > 0$ exists in this case. The shell cannot fall to the central singularity, because the gravitational field of the electric charge of the black hole produces such a high potential barrier that the kinetic energy of the falling shell is not enough to overcome it. The second inequality means that the energy of the shell tension is not enough to prevent the stop of shell contraction and subsequent expansion to infinity.

Potential (16) has a minimum at which, as was said above, it is always negative. Since the potential at infinity is also negative, the shell expands to an infinite radius in the long run. It can be shown that the inequality

$$\rho_{\text{in}}^+ > \rho_{\text{out}}. \quad (28)$$

will always hold in this case. This also means that only the characteristic radii ρ_{out}^- , ρ_{in}^- and ρ_{out} can change places in this case. For a more detailed description, let us divide this case into two subcases (Ia and Ib), depending on the relation $\rho_{\text{out}}^- \gtrless \rho_{\text{out}}$.

In the first subcase (Ia) corresponding to the condition

$$\rho_{\text{out}}^- > \rho_{\text{out}}, \quad (29)$$

or, equivalently, the condition

$$8\pi^2 A^2 < (m_{\text{out}} - m_{\text{in}}) \left(m_{\text{out}} - \sqrt{m_{\text{out}}^2 - Q^2} \right), \quad (30)$$

the characteristic radii will be located in the following order: $\rho_{\text{out}} < \rho_{\text{out}}^- < \rho_{\text{in}}^- < \rho_{\text{in}}^+ < \rho_{\text{out}}^+$, as shown in Fig. 2a. together with the plot of $U(\rho)$. The Carter–Penrose diagram corresponding to this case is presented in Fig. 3a. On this diagram, we see that, having begun its contraction from infinity in the R_+ region, the shell collapses (i.e., crosses the outer event horizon of the black hole) and falls into the T_- region. While continuing to contract, the shell then falls into the inner R_+ region, where it is reflected from the potential at the bounce point and begins to expand to infinity into a new outer R_+ region, passing through the T_+ region on its way.

The second subcase (Ib) corresponds to a change in the relative positions of the radius ρ_{out} and the event horizon ρ_{out}^- . This occurs when the condition $(m_{\text{out}} - m_{\text{in}}) \left(m_{\text{out}} - \sqrt{m_{\text{out}}^2 - Q^2} \right) = 8\pi^2 A^2$ is met. Thus, for the second subcase corresponding to the satisfaction of the condition

$$\rho_{\text{in}}^- > \rho_{\text{out}} > \rho_{\text{out}}^-, \quad (31)$$

the characteristic radii will be located in the following order: $\rho_{\text{out}}^- < \rho_{\text{out}} < \rho_{\text{in}}^- < \rho_{\text{in}}^+ < \rho_{\text{out}}^+$, as shown in Fig. 2b. The corresponding Carter–Penrose diagram is presented in Fig. 3b. In this case, the shell either expands infinitely or initially contracts, going below the event horizon, and subsequently expands to infinity but now in a different universe.

It remains to consider yet another case (Ic) where

$$\rho_{\text{out}} > \rho_{\text{in}}^- \quad (32)$$

or, equivalently,

$$(m_{\text{out}} - m_{\text{in}}) \left(m_{\text{in}} - \sqrt{m_{\text{in}}^2 - Q^2} \right) < 8\pi^2 A^2. \quad (33)$$

The characteristic radii will now be located in the following order: $\rho_{\text{out}}^- < \rho_{\text{in}}^- < \rho_{\text{out}} < \rho_{\text{in}}^+ < \rho_{\text{out}}^+$, as in Fig. 2c. The Carter–Penrose diagram will not change compared to the previous subcase. As we see from the plots of the potential, there are no stable, i.e., oscillating solutions for the shell in this case. The shell always expands to infinity for any initial parameters of the problem. The general solution for the shell evolution with the initial condition $\tau = 0$ at $\rho = \rho_0^-$ that corresponds to the subcase under consideration will be written as

$$\tau \sqrt{\frac{(m_{\text{out}} - m_{\text{in}})^2}{16\pi^2 A^2} - 1} - \sqrt{(\rho - \rho_0^-)(\rho - \rho_0^+)} = \frac{\rho_0^+ + \rho_0^-}{2} \ln \left\{ \frac{2 \left[\rho + \sqrt{(\rho - \rho_0^-)(\rho - \rho_0^+)} \right] - \rho_0^- - \rho_0^+}{\rho_0^- - \rho_0^+} \right\}.$$

Another case (II) is realized when the conditions $4\pi^2 A^2 < Q^2$ ($(m_{\text{out}} - m_{\text{in}})^2 < 16\pi^2 A^2$) are met.

As will be shown below, when these conditions are met, stable regular motions of the shell take place. The shell will execute oscillatory motions. This is because the energy of the shell tension is enough to reverse the motion of the shell at the bounce points due to the second inequality. We will also consider all possible subcases.

In the first subcase (IIa), the condition

$$\rho_{\text{out}} < \rho_{\text{out}}^- \quad (34)$$

is met. The characteristic radii are located in the following order: $\rho_{\text{out}} < \rho_{\text{out}}^- < \rho_{\text{in}}^- < \rho_{\text{in}}^+ < \rho_{\text{out}}^+$ as shown Fig. 4a together with the plot of the potential. The Carter–Penrose diagrams for this case are shown in Fig. 5a.

The next possible subcase (IIb) corresponds to the conditions

$$\rho_{\text{out}}^- < \rho_{\text{out}} < \rho_{\text{in}}^-. \quad (35)$$

The characteristic radii are located in the following order: $\rho_{\text{out}}^- < \rho_{\text{out}} < \rho_{\text{in}}^- < \rho_{\text{in}}^+ < \rho_{\text{out}}^+$, as shown in Fig. 4b. The Carter–Penrose diagrams is presented in Fig. 5b.

The next two subcases (IIc and IId) are related to a change in the relative positions of the characteristic radii ρ_{out} with ρ_{in}^- and ρ_{in}^+ . In the subcase (IIc) where

$$\rho_{\text{in}}^- < \rho_{\text{out}} < \rho_{\text{in}}^+ \quad (36)$$

the characteristic radii will be located in the following order $\rho_{\text{out}}^- < \rho_{\text{in}}^- < \rho_{\text{out}} < \rho_{\text{in}}^+ < \rho_{\text{out}}^+$. Accordingly, in the opposite case where

$$\rho_{\text{in}}^+ < \rho_{\text{out}} < \rho_{\text{out}}^+, \quad (37)$$

the characteristic radii will be located in the sequence $\rho_{\text{out}}^- < \rho_{\text{in}}^- < \rho_{\text{in}}^+ < \rho_{\text{out}} < \rho_{\text{out}}^+$. The Carter–Penrose diagram remains the same as that in the previous case.

Finally, in the last possible subcase (IId),

$$\rho_{\text{out}}^+ < \rho_{\text{out}}. \quad (38)$$

In this case, the relative positions of the characteristic radii are: $\rho_{\text{out}}^- < \rho_{\text{in}}^- < \rho_{\text{in}}^+ < \rho_{\text{out}}^+ < \rho_{\text{out}}$. The potential for this case is plotted in Fig. 4c and the Carter–Penrose diagram is shown in Fig. 5c. As was said above, two bounce points of the shell corresponding to radii $\rho_0^- > 0$ and $\rho_0^+ > 0$ exist in this case. We clearly see from the diagrams that the shell will execute infinite oscillatory motions, successively passing from one R_+ region to another R_+ region. The corresponding general solution for the evolution of an oscillating shell with the initial condition $\tau = 0$ at $\rho = \rho_0^-$ will be written as

$$\tau \sqrt{1 - \frac{(m_{\text{out}} - m_{\text{in}})^2}{16\pi^2 A^2}} + \sqrt{(\rho_0^+ - \rho)(\rho - \rho_0^-)} = \frac{\rho_0^+ + \rho_0^-}{2} \left\{ \frac{\pi}{2} - \arctan \left[\frac{\rho_0^+ + \rho_0^- - 2\rho}{2\sqrt{(\rho_0^+ - \rho)(\rho - \rho_0^-)}} \right] \right\}.$$

The next (in order) case (III) arises when the conditions $4\pi^2 A^2 > Q^2$ and $(m_{\text{out}} - m_{\text{in}})^2 < 16\pi^2 A^2$ are met. Now, there are no extremum. The branch of the potential grows smoothly and crosses the axis $U = 0$ at point ρ_0^+

The second bounce point is absent and, accordingly, there is no oscillating solution. The shell will collapse in the long run. Even if the shell initially expanded, its expansion will inevitably change into its contraction, as can be clearly seen on the Carter–Penrose diagram. It can be shown that the inequality

$$\rho_{\text{in}}^- < \rho_{\text{out}}. \quad (39)$$

holds in this case. Three additional subcases are possible.

In the first subcase (IIIa),

$$\rho_{\text{out}}^+ < \rho_{\text{out}}. \quad (40)$$

The characteristic radii are located in the following order: $\rho_{\text{out}}^- < \rho_{\text{in}}^- < \rho_{\text{in}}^+ < \rho_{\text{out}}^+ < \rho_{\text{out}}$. The potential for this case is shown in Fig. 6a and the Carter–Penrose diagram is presented in Fig. 7a.

The second subcase (IIIb) is realized for

$$\rho_{\text{in}}^+ < \rho_{\text{out}} < \rho_{\text{out}}^+. \quad (41)$$

This case differs from the previous one only in that the radii ρ_{out} and ρ_{out}^+ change places and, hence, the relative positions of the characteristic radii are now the following: $\rho_{\text{out}}^- < \rho_{\text{in}}^- < \rho_{\text{in}}^+ < \rho_{\text{out}} < \rho_{\text{out}}^+$. The plot of the potential together with the positions of the characteristic radii is shown in Fig. 6b and the Carter–Penrose diagram is presented in Fig. 7b.

Finally, the third subcase (IIIc) corresponds to the condition

$$\rho_{\text{in}}^+ > \rho_{\text{out}}. \quad (42)$$

The Carter–Penrose diagram will not change compared to the previous case. The general solution with the boundary condition $\tau = 0$ at $\rho = \rho_0^+$ will be written in this case as

$$\tau \sqrt{1 - \frac{(m_{\text{out}} - m_{\text{in}})^2}{16\pi^2 A^2}} + \sqrt{(\rho_0^+ - \rho)(\rho - \rho_0^-)} = -\frac{\rho_0^+ + \rho_0^-}{2} \left\{ \frac{\pi}{2} + \arctan \left[\frac{\rho_0^+ + \rho_0^- - 2\rho}{2\sqrt{(\rho_0^+ - \rho)(\rho - \rho_0^-)}} \right] \right\}.$$

Yet another case (IV) is possible where the conditions $4\pi^2 A^2 > Q^2$ ($m_{\text{out}} - m_{\text{in}})^2 > 16\pi^2 A^2$ are met.

In this case, there are no bounce points and, hence, the pattern of shell motion cannot change. Depending on the initial conditions, the shell either expands infinitely or contracts from infinity and falls to the singularity.

IV. A POLYTROPIC SHELL

In this section, we will consider the dynamics of a shell with a polytropic equation of state that is described by the equation of motion (12) with a potential of the general form U (13). To analyze the possible types of shell motion, the equation of motion should be supplemented by the conditions for the signs of σ . (14) and (15). Although this potential is cumbersome, it has properties similar to those of the potential for a dust shell. Indeed, for the potential in the general case, we have the relations:

$$U(\rho_{\text{in}}^\pm) = - \left[2\pi\rho\mu(\rho_{\text{in}}^\pm) + \frac{(m_{\text{out}} - m_{\text{in}})}{4\pi\rho_{\text{in}}^{\pm 2}\mu(\rho_{\text{in}}^\pm)} \right]^2, \quad (43)$$

$$U(\rho_{\text{out}}^\pm) = - \left[2\pi\rho\mu(\rho_{\text{out}}^\pm) - \frac{(m_{\text{out}} - m_{\text{in}})}{4\pi\rho_{\text{out}}^{\pm 2}\mu(\rho_{\text{out}}^\pm)} \right]^2. \quad (44)$$

The values of this potential on the outer and inner event horizons are negative or zero, as in the dust case. The potential at the points of change in the sign of σ is

$$U(\rho_{\text{out}}) = 1 - \frac{2m_{\text{out}}}{\rho_{\text{out}}} + \frac{Q^2}{\rho_{\text{out}}^2} - \left[2\pi\rho\mu(\rho_{\text{out}}) - \frac{(m_{\text{out}} - m_{\text{in}})}{4\pi\rho_{\text{out}}^2\mu(\rho_{\text{out}})} \right]^2,$$

$$U(\rho_{\text{in}}) = 1 - \frac{2m_{\text{in}}}{\rho_{\text{in}}} + \frac{Q^2}{\rho_{\text{in}}^2} - \left[2\pi\rho\mu(\rho_{\text{in}}) + \frac{(m_{\text{out}} - m_{\text{in}})}{4\pi\rho_{\text{in}}^2\mu(\rho_{\text{in}})} \right]^2.$$

As in the case of a dust shell, it follows from the conditions for the potential being zero on the event horizon and at the characteristic radii ρ_{out} and ρ_{in} that ρ_{out} and ρ_{in} coincide with the corresponding radii of the black hole event horizons. All of the above properties of the potential are valid for an arbitrary equation of state of an ideal fluid. Specifying the equation of state in an explicit (polytropic) form will be needed only in calculating the first and second derivatives of the potential:

$$\frac{\partial U}{\partial \rho} = -\frac{2Q^2}{\rho^3} + \frac{m_{\text{out}} + m_{\text{in}}}{\rho^2} - \frac{B(m_{\text{out}} - m_{\text{in}})^2}{4\pi^2\rho^{2\gamma+5}\mu^3(\rho)} + 8\pi^2\rho\mu(\rho) \left[\mu(\rho) + \frac{2B}{\rho^{2\gamma}} \right], \quad (45)$$

$$\begin{aligned} \frac{\partial^2 U}{\partial \rho^2} = & -\frac{2(m_{\text{out}} + m_{\text{in}})}{\rho^3} + \frac{6Q^2}{\rho^4} + 8\pi^2 \left[\mu(\rho) + \frac{2B}{\rho^{2\gamma}} \right]^2 - 16\pi^2\mu(\rho) \left[\mu(\rho) + \frac{(2\gamma+1)B}{\rho^{2\gamma}} \right] \\ & - \frac{(m_{\text{out}} - m_{\text{in}})^2(2\gamma-1)}{4\pi^2\rho^{2\gamma+6}\mu^3(\rho)} - \frac{3(m_{\text{out}} - m_{\text{in}})^2B^2}{2\pi^2\rho^{4\gamma+6}\mu^4(\rho)}, \end{aligned} \quad (46)$$

where $B = kA^\gamma$. As a result, potential (13) for the equation of motion (12) of the shell in general form has the same characteristic features as the potential in the special case of a dust shell we considered. Consequently, the parameters of the problem at which an infinite oscillatory motion of the shell takes place also exist for the general case. For example, the case of $A = 0$ and $\gamma = 5/4$ can also be investigated analytically. However, since the final results are very cumbersome, we do not present them here. For this case, stable oscillatory shell motions will take place, in particular, at the following parameters of the problem: $m_{\text{in}} = 1$, $m_{\text{out}} = 1.01$, $B = 0.001$ and $Q = 0.5$. Accordingly, for a different case where $A = 0$ and $\gamma = 2$, an oscillatory shell motion will take place, for example, at the following parameters of the problem: $m_{\text{in}} = 1$, $m_{\text{out}} = 1.001$, $B = 0.005$ $Q = 0.9$.

V. CONCLUSIONS

We analyzed all possible types of dynamical evolution of a thin shell in the geometry of an eternally existing electrically charged black hole using a dust shell as an example. In contrast to the Schwarzschild geometry, in the case of an electrically charged black hole, apart from the solutions with shell collapse or infinite expansion, a peculiar oscillating solution corresponding to the successive shell passage from one universe to the next in an infinite series of universes inside the event horizon of the charged black hole also exists. As we see from the corresponding Carter–Penrose diagrams, a dust shell can travel infinitely in the inner universes of a charged black hole. In this case, the periodically alternating stops of shell contraction and expansion occur successively in different universes. Oscillating solutions also exist for an arbitrary equation of state of the shell.

Since the global geometries of a rotating Kerr black hole and an electrically charged Reissner–Nordström black hole are similar, an oscillatory motion of the shell is also possible in principle in the case of a rotating black hole. Interesting corollaries of the oscillating solutions can also manifest themselves in modelling a multiverse that either exists eternally or results from the evolution of an initially simple universe through a multiple quantum birth of baby universes and their subsequent quantum splitting into a set of individual universes (worlds) connected in a topologically complex way.

Oscillating shells may prove to be the simplest probes that connect the individual worlds in the multiverse. Indeed, an observer in our universe can say nothing about the fate of a collapsing shell. In the case of a Schwarzschild black hole, it will fall to the central singularity. However, if the black hole has a charge or an angular momentum, then the shell inside the black hole can bounce and expand into another universe without reaching the singularity. If the observer will somehow detect an expanding shell whose expansion will then change into contraction, then he can assume that this shell has come from another universe. Accordingly, electrically charged and rotating black holes with

bounce points inside their event horizons may prove to be the gates into other universes. Incomplete collapse with a bounce into another universe opens the fundamental possibility of the existence of objects from other universes in our universe.

The existence of solutions with a bounce into other universe is of fundamental importance for the quantization of black holes, quantum birth of baby universes, and quantum cosmology as a whole, because the necessity of taking into account the transitions between states in different universes arises at the quantum level.

Since there is no quantum theory of gravity, semiclassical models are a powerful tool for investigating quantum effects in strong gravitational fields. One of the most important present day problems is the problem of quantum tunnelling in the case of a multiverse. In particular, the question about the probability of particle tunnelling from one universe to another through a charged or rotating black hole arises. The oscillating solutions can be used to solve the problem of such tunnelling and to consider other properties of the quantum fields in the Reissner–Nordström metric in the semiclassical approximation.

Acknowledgments

This work was supported by the Russian Federal Agency for Science and Innovation under state contract 02.740.11.5092 and by the grants of the Leading scientific school 959.2008.2.

-
- [1] W. Israel, *Nuovo Cimento B* 44, 1 (1966).
 - [2] W. Israel, *Phys. Rev.*, 153, 1388 (1967).
 - [3] K. Kuchar, *Czech. J. Phys. B*, 18, 435 (1968).
 - [4] V. De La Cruz, W. Israel, *Phys. Rev.*, 170, 1187 (1968).
 - [5] S. K. Blau, E. I. Guendelman, A. H. Guth, *Phys. Rev. D* 35, 1747 (1987).
 - [6] V. A. Berezin, V. A. Kuzmin, I. I. Tkachev, *Phys. Rev. D* 36, 2919 (1987).
 - [7] D. A. Kirzhnits, *Pisma Zh. Eksp. Teor. Fiz.* 15 (12), 745 (1972) [*JETP Lett.* 15 (12), 529 (1972)].
 - [8] D. A. Kirzhnits, A. D. Linde, *Phys. Lett. B* 42, 471 (1972).
 - [9] K. Sato, M. Sasaki, H. Kodama, K. Maeda, *Phys. Lett. B* 108, 103 (1982).
 - [10] H. Kodama, *Prog. Theor. Phys.* 63, 1217 (1980).
 - [11] K. Sato, M. Sasaki, H. Kodama, K. Maeda, *Prog. Theor. Phys.* 65, 1443 (1981).
 - [12] H. Kodama, M. Sasaki, K. Sato, K. Maeda, *Prog. Theor. Phys.* 66, 2052 (1981).
 - [13] K. Sato, *Prog. Theor. Phys.* 66, 2287 (1981).
 - [14] H. Kodama, M. Sasaki, *Prog. Theor. Phys.* 68, 1398 (1982).
 - [15] M. Sasaki, H. Kodama, K. Sato, *Prog. Theor. Phys.* 68, 1561 (1982).
 - [16] H. Kodama, M. Sasaki, K. Sato, *Prog. Theor. Phys.* 68, 1979 (1982).
 - [17] K. Maeda, M. Sasaki, K. Sato, *Prog. Theor. Phys.* 69, 89 (1983).
 - [18] K. Maeda, H. Sato, *Prog. Theor. Phys.* 70, 772 (1983).
 - [19] Y. Suto, K. Sato, H. Sato, *Prog. Theor. Phys.* 71, 938 (1984).
 - [20] A. D. Dolgov, A. F. Illarionov, N. S. Kardashev, and I. D. Novikov, *Zh. Eksp. Teor. Fiz.* 94 (8), 1 (1988) [*Sov. Phys. JETP* 67 (8), 1517 (1988)].
 - [21] C. Barrabes, W. Israel, *Phys. Rev. D*, 43, 1129 (1991).
 - [22] V. A. Berezin, V. A. Kuzmin, I. I. Tkachev, *Phys. Lett. B* 120, 91 (1983).
 - [23] V. A. Berezin, V. A. Kuzmin, I. I. Tkachev, *Phys. Lett. B* 124, 479 (1983).
 - [24] V. A. Berezin, V. A. Kuzmin, I. I. Tkachev, *Phys. Lett. B* 130, 23 (1983).
 - [25] V. A. Berezin, V. A. Kuzmin, and I. I. Tkachev, *Pisma Zh. Eksp. Teor. Fiz.* 41 (10), 446 (1985) [*JETP Lett.* 41 (10), 547 (1985)].
 - [26] Ya. B. Zeldovich, I. Yu. Kobzarev, and L. B. Okun, *Zh. Eksp. Teor. Fiz.* 67 (1), 3 (1974) [*Sov. Phys. JETP* 40 (1), 1(1974)].
 - [27] I. Yu. Kobzarev, L. B. Okun, and M. B. Voloshin, *Yad. Fiz.* 20 (6), 1229 (1975) [*Sov. J. Nucl. Phys.* 20 (6), 644 (1975)].
 - [28] S. Coleman, *Phys. Rev. D* 15, 2929 (1977).
 - [29] C. G. Callan, S. Coleman, *Phys. Rev. D* 16, 1762 (1977).
 - [30] S. Coleman, F. De Luccia, *Phys. Rev. D* 21, 3305 (1980).
 - [31] K. Maeda, *Gen. Rel. Grav.*, 18, 931 (1986).
 - [32] V. A. Berezin, V. A. Kuzmin, and I. I. Tkachev, *Zh. Eksp. Teor. Fiz.* 86 (3), 785 (1984) [*Sov. Phys. JETP* 59 (3), 459 (1984)].
 - [33] A. Aurilia, G. Denardo, F. Legovivni, E. Spallucci, *Phys. Lett. B* 147, 258 (1984).
 - [34] A. Aurilia, G. Denardo, F. Legovivni, E. Spallucci, *Nucl. Phys. B* 252, 523 (1985).

- [35] A. Aurilia, M. Palmer, E. Spallucci, *Phys.Rev. D* 40, 2511 (1989).
- [36] A. Aguirre, M. C. Johnson, *Phys. Rev. D* 72, 103525 (2005).
- [37] J. Kijowski, G. Magli, D. Malafarina, *Gen. Rel. Grav.*, 38, 1697 (2006).
- [38] V. I. Dokuchaev and S. V. Chernov, *Pisma Zh. Eksp. Teor. Fiz.* 85 (12), 727 (2007) [*JETP Lett.* 85 (12), 595 (2007)].
- [39] V. I. Dokuchaev and S. V. Chernov, *Zh. Eksp. Teor. Fiz.* 134 (2), 245 (2008) [*JETP* 107 (2), 203 (2008)].
- [40] S. V. Chernov, V.I. Dokuchaev, *Class. Quant. Grav.* 25, 015004 (2008).
- [41] M. V. Barkov, V. A. Belinski, and G. S. Bisnovaty-Kogan, *Zh. Eksp. Teor. Fiz.* 122 (3), 435 (2002) [*JETP* 95 (3), 371 (2002)].
- [42] L. F. Abbott, S. Coleman, *Nucl. Phys. B*, 259, 170 (1985).
- [43] W. Lee, B.-H. Lee, C. H. Lee, C. Park, *Phys. Rev. D*, 74, 123520 (2006).
- [44] W. Lee, B.-H. Lee, C. H. Lee, S. Nam, C. Park, *Phys. Rev. D*, 77, 063502 (2008).
- [45] W. Lee, B.-H. Lee, S. Nam, C. Park, *Phys. Rev. D*, 75, 103506 (2007).
- [46] V. A. Berezin, *Fiz. Elem. Chastits At. Yadra* 34, 49 (2003).
- [47] V. A. Berezin, *Phys. Rev. D*, 55, 2139 (1997).
- [48] V. A. Berezin, A. M. Boyarsky, A. Yu. Neronov, *Phys. Rev. D*, 57, 1118 (1998).
- [49] V. A. Berezin, A. M. Boyarsky, A. Yu. Neronov, *Phys. Lett. B*, 455, 109 (1999).
- [50] V. A. Berezin, [ArXiv:gr-qc/0112022](https://arxiv.org/abs/gr-qc/0112022).
- [51] V. A. Berezin, N. G. Kozimirov, V. A. Kuzmin, I. I. Tkachev, *Phys. Lett. B*, 212, 415 (1988).
- [52] V. A. Berezin, *Phys. Lett. B*, 241, 194 (1990).
- [53] V. Berezin, V. Dokuchaev, Yu. Eroshenko, A. Smirnov, *Class. Quant. Grav.* 22, 4443 (2005).
- [54] V. Berezin, M. Okhrimenko, *Class. Quant. Grav.*, 18, 2195 (2001).
- [55] I. Guendelman, I Shilon, *Class. Quant. Grav.*, 26, 045007 (2009).
- [56] I. D. Novikov, *Astron. Zh.* 43, 911 (1966) [*Sov. Astron.* 43, 731 (1967)].
- [57] V. A. Berezin, V. A. Kuzmin, and I. I. Tkachev, *Zh. Eksp. Teor. Fiz.* 93 (4), 1159 (1987) [*Sov. Phys. JETP* 66 (4), 654 (1987)].
- [58] S. Chandrasekhar, *The Mathematical Theory of Black Holes* (Oxford University Press, Oxford, 1983; Mir, Moscow, 1986), p. 209.
- [59] R. F. Tooper, *Astrophys. J.*, 142, 1541 (1965).
- [60] Ya. B. Zeldovich, *Zh. Eksp. Teor. Fiz.* 41, 1609 (1961) [*Sov. Phys. JETP* 14, 1143 (1961)].

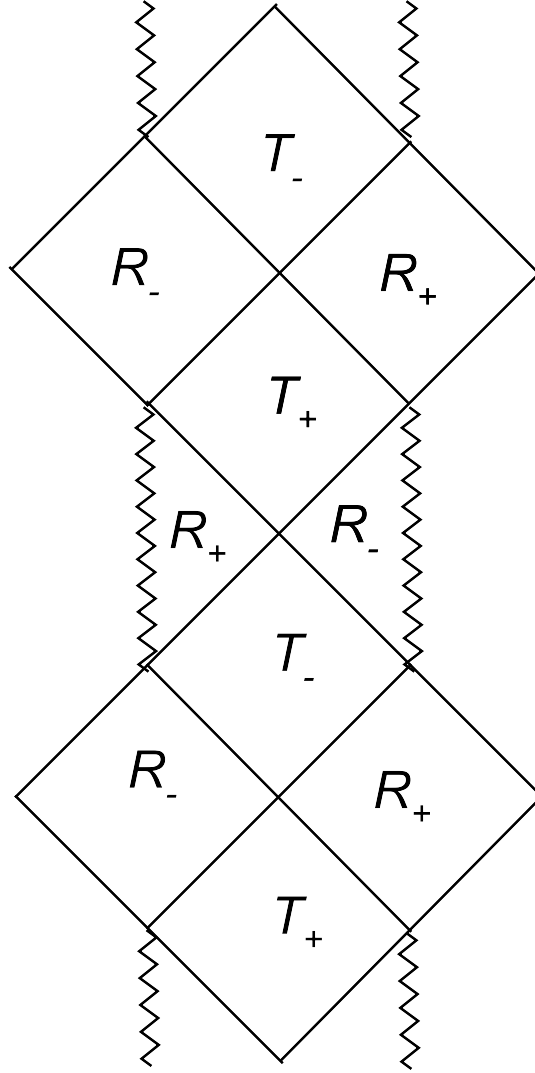


FIG. 1: The Carter-Penrose diagrams for the metric of an eternal Reissner-Nordström black hole (without a shell). The global geometry of an eternal electrically charged black hole is an infinite series of identical universes with time-like singularity (indicated by the polygonal line). The R_{\pm} and T_{\pm} spacetime regions are shown.

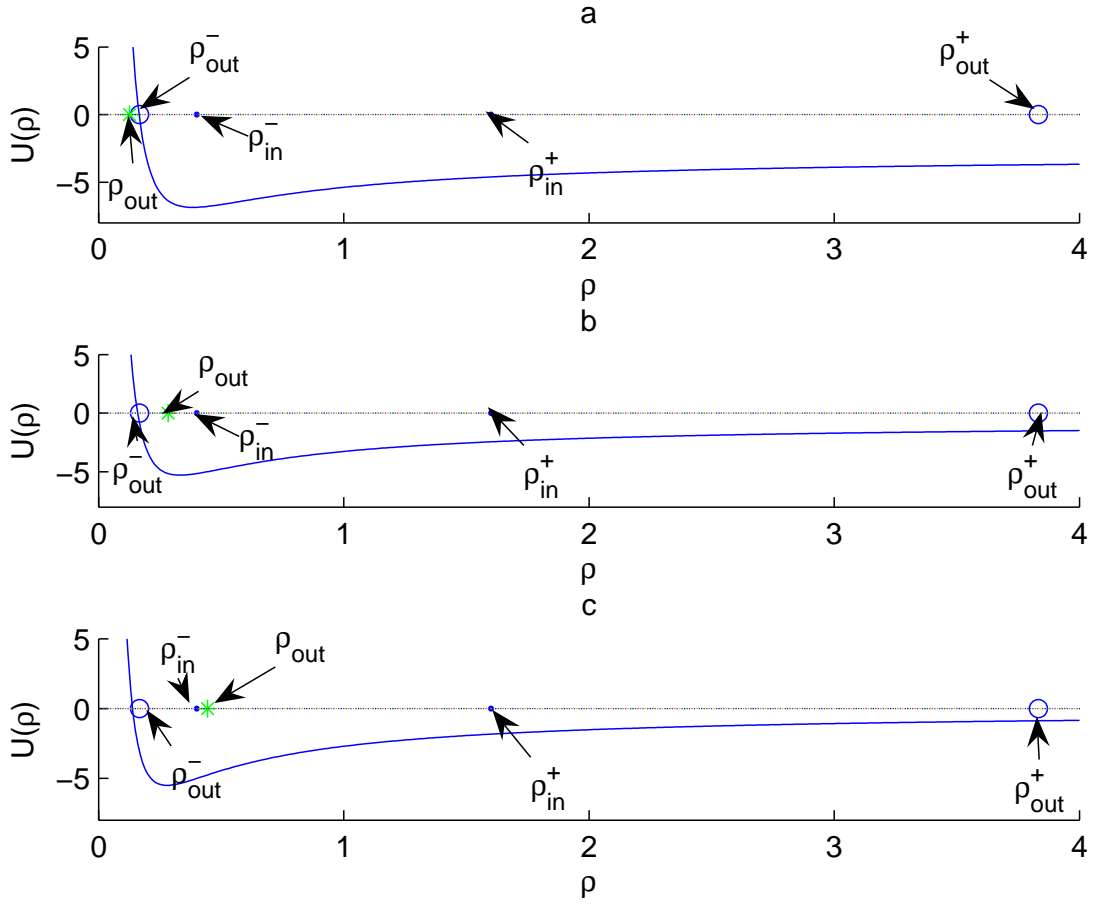


FIG. 2: Plots of the potentials and positions of the characteristic radii at $m_{\text{out}} = 2$, $m_{\text{in}} = 1$ and $Q = 0.8$ for the following cases: (a) $\rho_{\text{out}}^{-} > \rho_{\text{out}}$ at $A = 0.04$; (b) $\rho_{\text{in}}^{-} > \rho_{\text{out}} > \rho_{\text{out}}^{-}$ at $A = 0.06$ and (c) $\rho_{\text{out}} > \rho_{\text{in}}^{-}$ at $A = 0.075$.

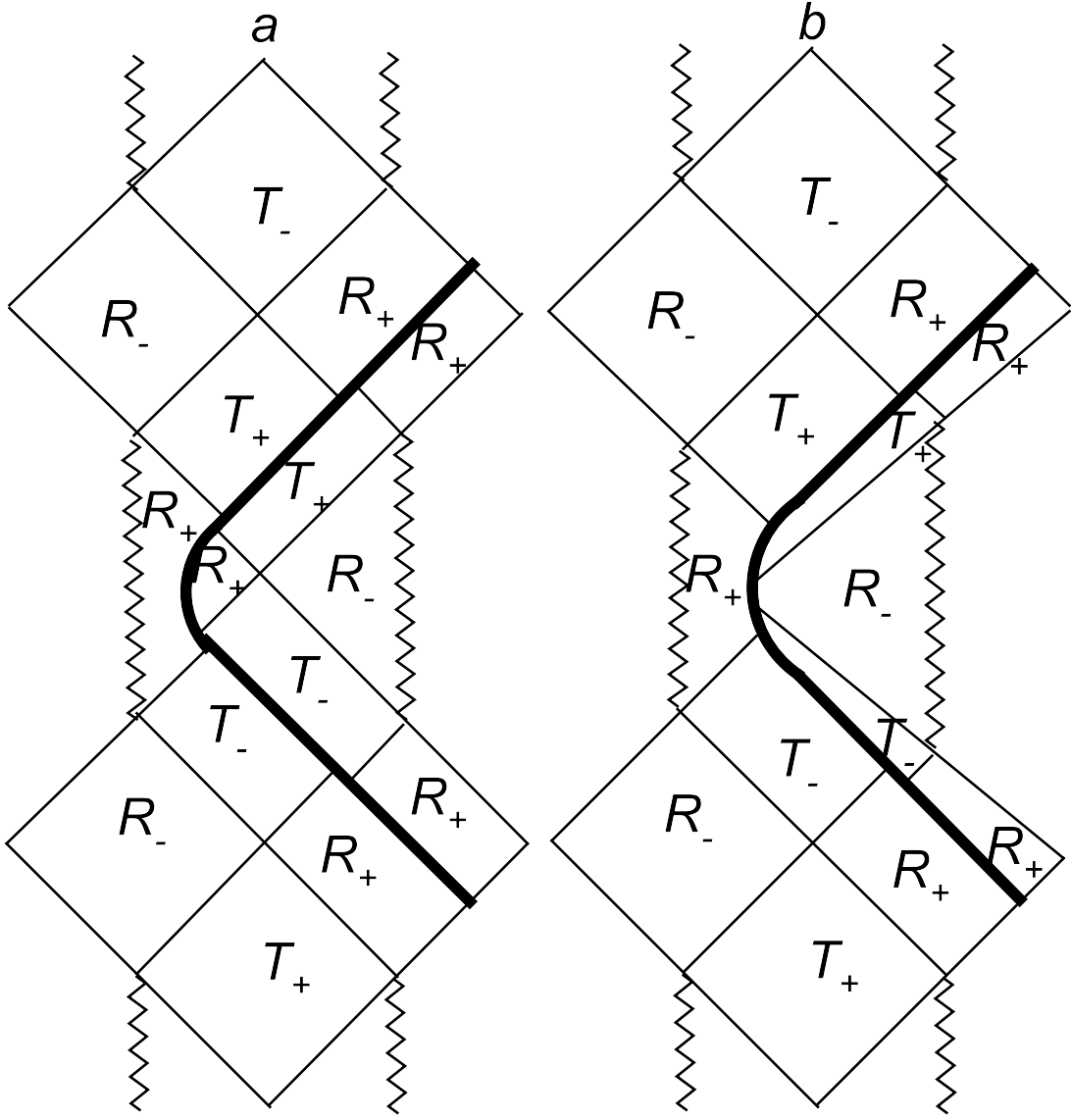


FIG. 3: Carter-Penrose diagrams for the following cases: (a) $\rho_{\text{out}}^- > \rho_{\text{out}}$ and (b) $\rho_{\text{out}} > \rho_{\text{out}}^-$.

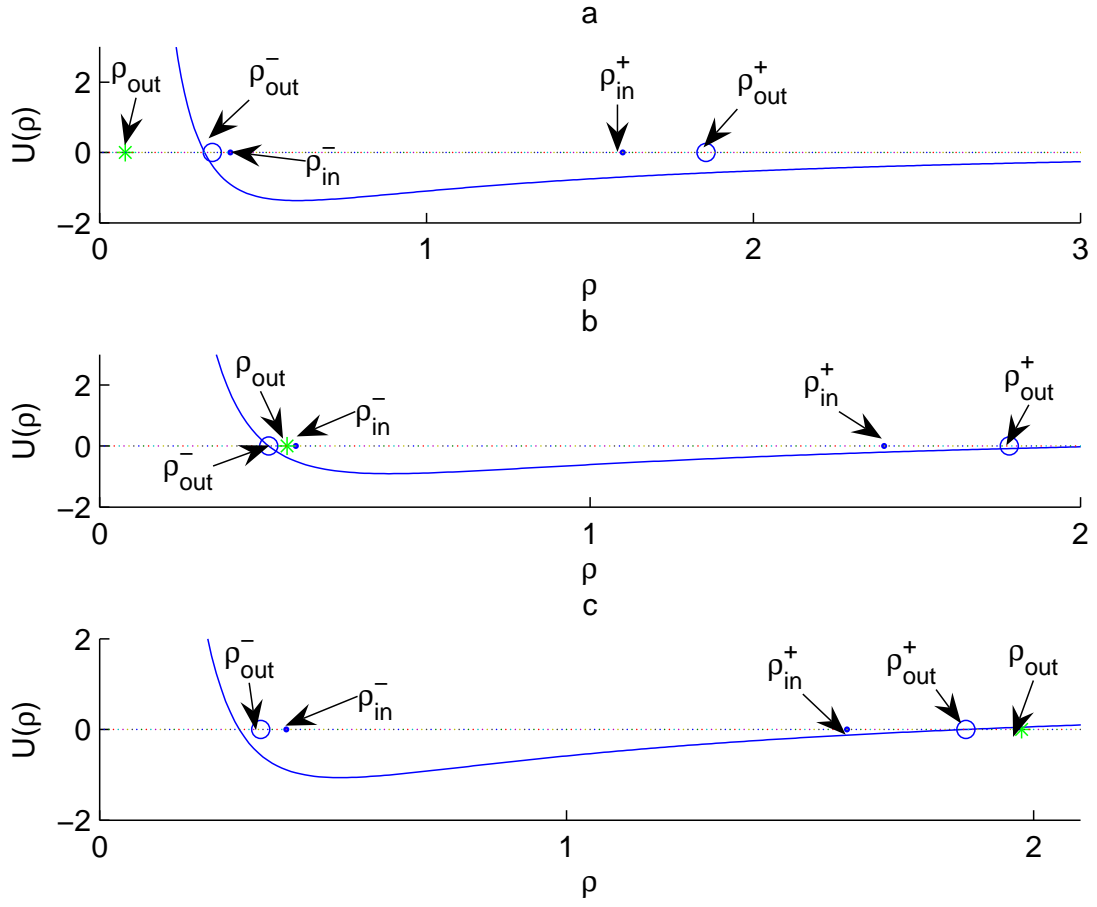


FIG. 4: Effective potential $U(\rho)$ and relative positions of the characteristic radii at $m_{out} = 1.1$, $m_{in} = 1$ and $Q = 0.8$ for the following possible cases: (a) $\rho_{out} < \rho_{out}^-$ at $A = 0.01$; (b) $\rho_{out}^- < \rho_{out} < \rho_{out}^+$ at $A = 0.022$ and (c) $\rho_{out}^+ < \rho_{out}$ at $A = 0.05$.

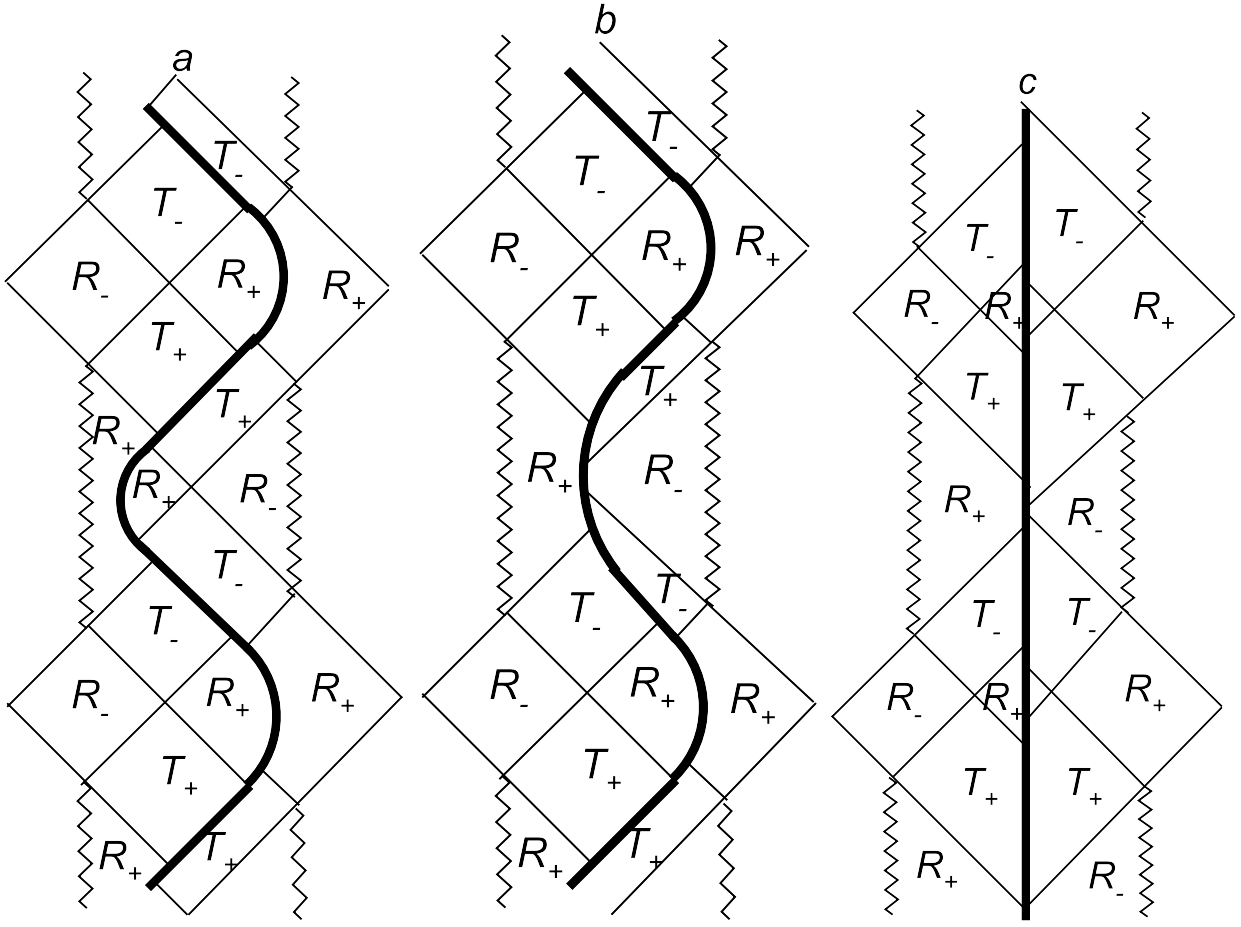


FIG. 5: The Carter-Penrose diagrams for the following cases: (a) $\rho_{\text{out}} < \rho_{\text{out}}^-$; (b) $\rho_{\text{out}}^- < \rho_{\text{out}} < \rho_{\text{out}}^+$ and (c) $\rho_{\text{out}}^+ < \rho_{\text{out}}$.

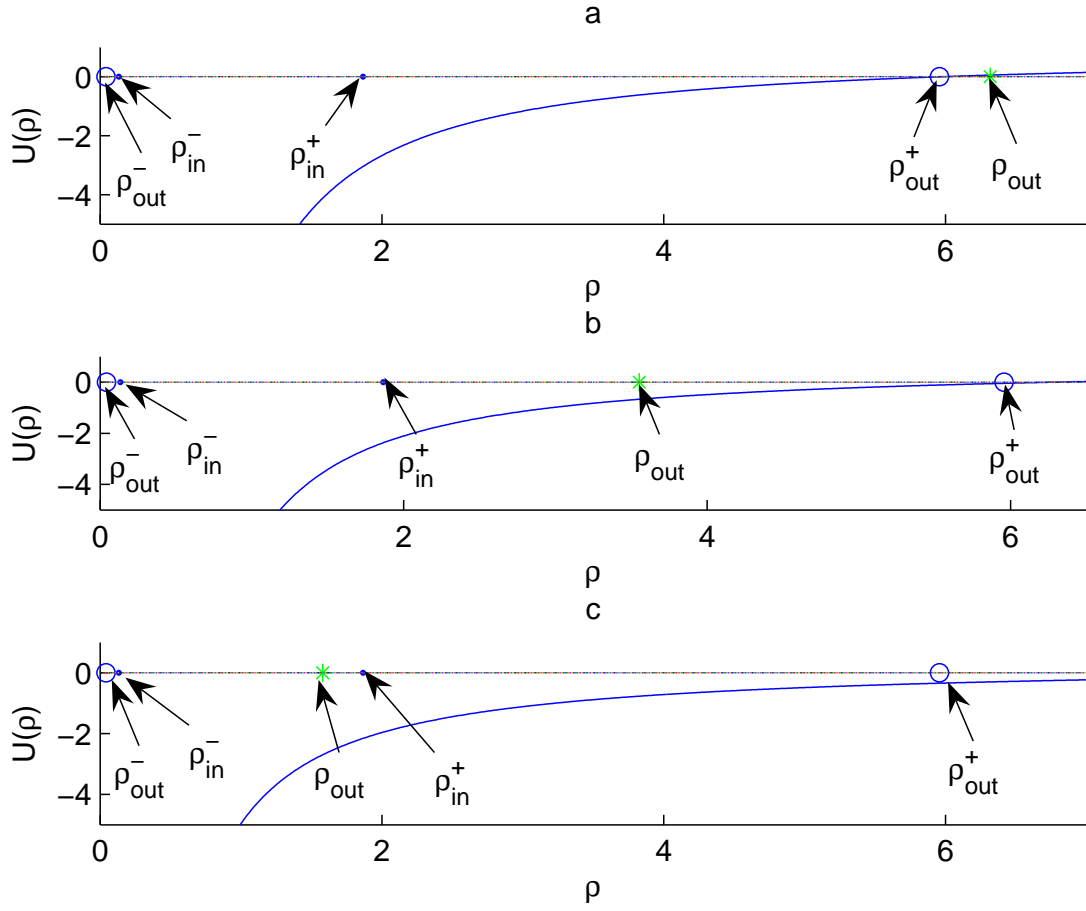


FIG. 6: Relations $U(\rho)$ and relative positions of the characteristic radii at $m_{out} = 3$, $m_{in} = 1$ and $Q = 0.5$ for the following cases: (a) $\rho_{out} > \rho_{out}^+$ at $A = 0.4$; (b) $\rho_{out}^+ > \rho_{out} > \rho_{in}^+$ at $A = 0.3$ and (c) $\rho_{in}^+ > \rho_{out}$ at $A = 0.2$.

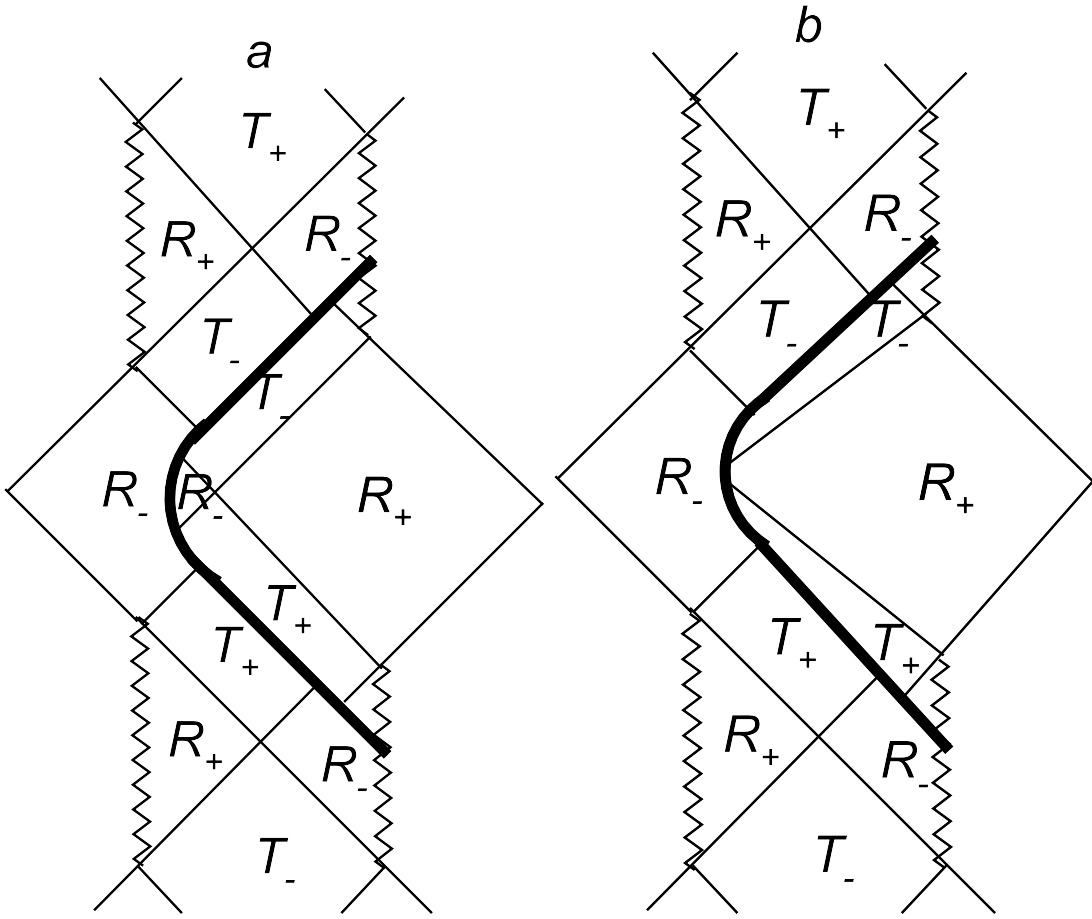


FIG. 7: The Carter-Penrose diagrams for the following cases: (a) $\rho_{\text{out}} > \rho_{\text{out}}^+$ and (b) $\rho_{\text{out}}^+ > \rho_{\text{out}}$.